



# 2D SPH simulation of an anaerobic digester

Prashant Kumar<sup>1</sup> · Soroush Dabiri<sup>1</sup> · Wolfgang Rauch<sup>1</sup>

Received: 21 June 2021 / Revised: 4 March 2022 / Accepted: 5 March 2022 / Published online: 2 April 2022  
© The Author(s) 2022

## Abstract

Understanding the hydrodynamics within the anaerobic digester tank of a wastewater treatment plant is of high importance to ensure sufficient mixing and subsequently a homogeneous distribution of the substrates. In this paper, we demonstrate a two-dimensional computational fluid dynamics simulation of a real-world case study focusing on both, the methodology and the operation of mixing. For this work, DualSPHysics, a Lagrangian solver, has been explored as an alternative to the more commonly used Eulerian solvers in studying the slow-moving dynamics inside a digester tank. This choice of a Lagrangian solver is primarily due to the inherent accounting for advection within the formulation, thus allowing for subsequent modelling of anaerobic digestion processes. A comparison has been made between the simulations from the two methods (Eulerian and Lagrangian), highlighting the benefits and the shortcomings of using smoothed particle hydrodynamics. Concerning operational mixing, the case relies on a draft tube, the effect of which on the velocity profiles has been studied based on the presence of low-velocity zones and Lagrangian coherent structures. Removing the draft tube results in an increase in low-velocity zones by 21.38% while the amount of dead volume increases from 0.52 to 1.2%.

**Keywords** Smooth particle hydrodynamics · Waste water treatment · Computational fluid dynamics · Draft tube · Low-velocity zone

## 1 Introduction

In the course of wastewater treatment (WWT), it is common practice to handle the resulting sludge from the biological processes by means of anaerobic digestion (AD). We denote AD as the biochemical degradation of organic matter by microorganisms, resulting in the production of a methane rich gas. As compared to other options for sludge management, the main advantage of AD is when used as a bare-bones process, the production of energy via methane gas instead of utilisation. Thus, the analysis, simulation and possible optimisation of the AD process has been a matter of scientific interest for decades.

The most coherent model for simulating the biochemical processes within the digester tank is denoted Anaerobic

Digestion Model No1 (ADM1) and has been presented by Batstone et al. [1]. The model considers AD as an amalgamation of the four main components: liquid phase, gas phase, physiochemical reactions and biological reactions. The formulated equations for each of which are solved separately.

Although ADM1 is accepted as a standard for modelling the biokinetic process within a sludge reactor, it does not give a complete representation of the physics due to its neglect of hydrodynamics when solving for the liquid phase. This is because, for the purpose of simplifications, ADM1 assumes the digester as a continuously stirred tank reactor, thus, implying the homogeneity of the sludge and uniform temperature conditions [11,13]. This leads to the model having compromised accuracy when representing the system.

In light of the above, computational fluid dynamics (CFD) can be useful to improve the accuracy of AD models by capturing the hydrodynamic flow field. Despite the rather low flow velocities of the sludge inside the tank, efficient mixing of the fluid is required to ensure optimal conditions for biodegradation and methane production, i.e., the homogeneity of both mixed liquor and fluid temperature as well as the prevention of both sedimentation and the floating sludge [19,25]. Appropriate mixing has to be enforced by either one or a combination of the following,

✉ Prashant Kumar  
prashant.kumar@uibk.ac.at

Soroush Dabiri  
soroush.dabiri@uibk.ac.at

Wolfgang Rauch  
woufgang.rauch@uibk.ac.at

<sup>1</sup> Universität Innsbruck Unit of Environmental Engineering,  
Technikerstraße 13, Room 311, 6020 Innsbruck, Austria

- mechanical mixing devices, i.e., impellers, propellers or draft tubes.
- sludge recirculation including optimal design of inlet configurations which also serves for temperature management via external heating.
- gas injection, i.e., utilising the gas bubbles resulting from the AD process to enforce an upward flow field.

Simulations to study the hydrodynamics of a digester have been done in the past, however, they are limited to the use of Eulerian methods. For example, Moulic et al. [18] used an Eulerian–Eulerian two-phase modelling approach to simulate a digester with gas injection. The effect of different turbulence models on the retention time was simulated by means of particle tracking. Kostoglou et al. [14] used a two-dimensional CFD framework to study the effectiveness of flotation tanks in WWT which do not make use of forced mixing due to mechanical mixing or recirculation. They found that bubbles and particles between 30 mm and 200 mm have a substantial effect on the flow dynamics when there is no external agitation. Terashima et al. [24] conducted a three-dimensional CFD simulation for a full-scale anaerobic digester and compared their results to tracer measurements. They used the temporal and spatial distribution of the tracer to describe a Uniformity Index which indicates the degree of mixing within the reactor. They verified that the index increased with mixing intensity

It is safe to assume that Eulerian CFD modelling is the industry standard for hydrodynamic simulations in AD. Despite the prevalence and the advantages of the fixed mesh approach, it has its own set of problems, such as the substantial increase in computational power required for transient simulations, the problems in dealing with phase boundaries in free-surface and multiphase flows along with the ensuring the quality of the mesh [9]. An imperative aspect of AD modelling is the use of biokinetic components which in the Eulerian framework requires to account for both the advection and the diffusion components. While possible, the latter requirements limit the application power of Eulerian approaches for integrated AD simulations (coupling hydrodynamics with biokinetic conversion).

The other approach is the use of a Lagrangian technique to simulate the flow field as done in the smoothed particle hydrodynamics (SPH) framework. It is a meshless approach where the fluid is discretized into particles that move according to force fields. This circumvents a majority of the limitations of a mesh-based solver. The main features and advantages of the approach as compared to standard solutions are summarised as follows;

- particles represent the properties of the fluid
- particles conserve mass while the advection in the transport phenomena is inherently accounted for via the movement of the particles

- free-surfaces and the phase boundaries can be easily tracked with the particles allowing for modelling interfacial flow problems
- coupling the hydrodynamics of the system with the biokinetic process can be done directly, based on particles representing a certain mass fraction of the fluid [26].

A potential disadvantage of SPH compared to Eulerian solvers is that the former is inherently transient and not efficient if aiming for computing steady-state hydrodynamics.

This work makes use of DualSPHysics (DSPH), a Lagrangian solver as presented in Domínguez et al. [5] to simulate the hydrodynamics of a digester. The work presented herein is to be seen as the first and fundamental step to develop a coherent framework to simulate the AD process as coupled hydrodynamic–biokinetic process. Such an integrated approach is necessary to compute the effect of the fluid behaviour on methane production in anaerobic digestion.

A similar effort was done by Winkler et al. [26] by applying a two-dimensional code called Smoothed Particle Hydrodynamics Activated Sludge Engine (SPHASE) [27]. Despite its applicability, SPHASE was hard-coded for the specific geometry of the tank in question and the biokinetic processes, thus making modifications to the geometry a tedious task. Moreover, the code structure made it necessary to misrepresent the tank due to the setup of periodic boundary conditions. Despite these shortcomings, SPHASE established a baseline against which the DSPH simulation can be compared and validated.

The aim of this work is to make use of DSPH to simulate the hydrodynamics within an anaerobic digestion tank. The low velocities and the requirement to simulate for longer periods make this problem not particularly well suited for such a framework, however, as stated earlier, using SPH would be of immense advantage when working with the biokinetic models for AD processes. We also aim to use the specified methodology to evaluate the effect of the removal of an external mixing device, i.e., the draft tube on the flow dynamics within the tank. We will compare the results obtained with Eulerian (Ansys FLUENT) simulations and comment on the mixing characteristics of the multiple configurations of tanks. This will be based on the velocity contours, presence of low-velocity zones (LVZ) and dead volume and identifying Lagrangian coherent structure (LCS) to generalize the flow pattern.

## 2 Methodology

SPH for fluid dynamics considers the fluid domain to be discretized into separate particles, each of which has its own set of properties maintaining its own time history. These particles move according to the solution of the discretized momentum and continuity equations.

### 2.1 Governing equations for SPH

A particular quantity  $A$  for a particle,  $a$ , located at distance  $\mathbf{r}$  from another particle,  $b$ , in integral form is given by

$$A(\mathbf{r}) = \int A(\mathbf{r}')W(\mathbf{r} - \mathbf{r}', h)d\mathbf{r}' \tag{1}$$

However, in its discretized form, the aforementioned equation can be expressed as

$$A(\mathbf{r}) = \sum_b m_b \frac{A_b}{\rho_b} W(\mathbf{r}), \tag{2}$$

where  $m$  and  $\rho$  denote the mass and density of their respective particles. The particle  $b$  is chosen such that it is within the support group of the first particle, as defined by the kernel function,  $W(\mathbf{r})$ .

**Kernel function** The solution to the earlier equation is based on the properties of the neighbouring particles as specified by the smoothing length [16]. The smoothing length is the distance that demarcates the support group for the *particle under consideration*. A kernel function [2], which is a compact support function of the distance,  $\mathbf{r}$  between the two particles and the smoothing length,  $h$ , delineates the influence of the neighbouring particles on the particle.

**Continuity equation** The differential form of the continuity equation is given by,

$$\frac{d\rho}{dt} = -\rho \nabla \cdot \mathbf{v} \tag{3}$$

where  $\rho$  is the fluid density and  $\mathbf{v}$  is the flow velocity. It can then be discretized as

$$\frac{d\rho_a}{dt} = \rho_a \sum_b \frac{m_b}{\rho_b} \mathbf{v}_{ab} \cdot \nabla_a W_{ab} \tag{4}$$

where  $\mathbf{v}_{ab}$  is the relative velocity between particles  $a$  and  $b$ . This is utilised to calculate the fluctuating densities, a product of the properties of weakly compressible simulations [27].

However, the simulations in Sects. 4.2 and 4.3 make use of the density diffusion terms to help alleviate the numerical noise frequently visible in the pressure field. DSPH allows the use of density diffusion formulation for this purpose. This results in the aforementioned continuity equation having a form as given by Fourtakas et al. [10, section 3.2].

**Momentum equation** The momentum equation [6,17] for a continuous medium is defined as

$$\frac{d\mathbf{v}}{dt} = -\frac{1}{\rho} \nabla p + \frac{\mathbf{F}^v}{\rho} + \mathbf{g}, \tag{5}$$

where  $p$  represents the pressure and  $\mathbf{F}^v$  represents the dissipative forces.

In SPH formulation, this equation changes for particle  $a$  to

$$\frac{d\mathbf{v}_a}{dt} = -\sum_b m_b \left( \frac{p_b + p_a}{\rho_a \rho_b} + \Pi_{ab} \right) \nabla_a W_{ab} + \mathbf{g}. \tag{6}$$

The viscous term  $\Pi_{ab}$  is given by

$$\frac{-\alpha(c_a + c_b)\mu_{ab}}{\rho_a + \rho_b} \text{ when } \mathbf{v}_{ab} \cdot \mathbf{r}_{ab} < 0, \tag{7}$$

where

$$\mu_{ab} = \frac{h\mathbf{v}_{ab} \cdot \mathbf{r}_{ab}}{(\mathbf{r}_{ab}^2 + 0.01h^2)}. \tag{8}$$

Further information about the SPH formulation such as boundary conditions and time stepping can be found in Domínguez et al. [5].

### 2.2 Mixing characteristics

There are various methods and criteria available which can be used to characterise mixing. One of the criteria, which is useful in digester hydrodynamics, is governed by the presence of low-velocity zones(LVZ) and dead volume within the tank [28]. Regions with the velocity magnitude ranging from  $0.001 \text{ ms}^{-1}$  to  $0.01 \text{ ms}^{-1}$  are termed as LVZ and dead volumes have a velocity magnitude of less than  $0.001 \text{ ms}^{-1}$ . The benefit of using this approach is that this is one of the few criteria which can be compared to experimental tests by comparing the dead volume found during tracer measurements in the digester tanks.

When considering simulations, having dead volume within the tank means that the velocities are too low for efficient mixing of the bio-waste [3,22]. This, on the one hand, leads to low methane yield and on the other hand, the accumulation of sediments in the tank results in a reduction of the available volume. Operators aim to reduce lvz and to prevent or minimize the dead volume within the tank.

Another important mixing criterion in the case of SPH is the finite time Lyapunov exponent (FTLE), ( $\sigma$ ), and the identification of Lagrangian coherent structure (LCS) [23]. FTLE is a scalar value for each of the particles of the fluid and represents how the average trajectory of the particle stretches over a given time. Unlike velocity profiles or streamlines, FTLE is time-averaged hence the contours do not decay over time for the case of time-dependent flows. They instead provide a basic skeletal structure along which the flow develops, i.e., in the Lagrangian context, an indication if the particles would diverge or converge in a particular region.

Our formulation of FTLE at time  $T$  is based on the works of Reece et al. [20] using

$$\sigma_a = \frac{1}{T} \ln \left[ \sqrt{\max_b \frac{|r_{ab}(t=T)|}{|r_{ab}(t=0)|}} \right] \quad (9)$$

where the maximum distance between all the particles within the support of particle  $a$  is considered.

Plotting the FTLE within the geometry shows the formation of LCS within the fluid. The FTLE can either be forward or backward based on the direction movement over time. A forward FTLE means that the LCS formed repels the fluid and forms *ridges* within it. On the other hand, an LCS based on backward FTLE form *valleys* and attract the fluid within its vicinity. This implies that if a tracer is introduced close to a ridge, it would move away from the LCS and will not cross over. The separation formed might lead to inefficient mixing with the substrate not being able to interact with certain regions of the tank. This can be a cause for concern as these regions could possibly suffer from suboptimal biokinetic reaction rates.

### 3 Case setup

Figure 1a shows the two-dimensional cross-sectional geometry of the digester tank at a WWT facility in Tirol, Austria [15]. While it is clear that a two-dimensional model of the true reactor geometry is not accurately describing the hydrodynamics, implementation of a three-dimensional model is not possible due to the size of the tank, thus resulting in unrealistic computational times. Furthermore, the previous simulation by Rezavand et al. [21], which is used to validate the simulation, was also done in a two-dimensional scale.

The tank is 24 m in height with a diameter of 15.4 m and a total capacity of approximately 2500 m<sup>3</sup>. The feed velocity, based upon the flow rate, is taken as 0.95 ms<sup>-2</sup>. Under normal working conditions, the tank is filled to a height of 22.9 m which is taken as the effective height of the digester in the first geometry. Regarding flow characteristics, it is to be noted that experimentally determining the flow velocities within the tank is next to impossible and thus the Reynolds number can only be estimated. However, based on the geometry and the readily available inflow conditions, the flow inside is highly turbulent with an approximate Reynolds number of 48 000. Such a high Reynolds number is primarily due to the large size of the digester even though the average velocity inside is in the order of 0.03 m s<sup>-1</sup> despite having external mixing introduced using the draft tube.

In this case study, mixing is provided by both a recirculation flow and a draft tube. The latter constitutes of a pipe, 0.35 m in diameter that houses an impeller creating an

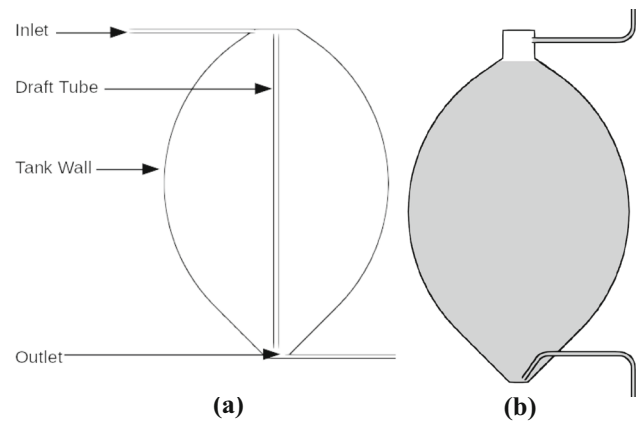


**Fig. 1** Geometries of the tank used for the simulations **a** initial (simplified) digester geometry—see Rezavand et al. [21] **b** modified tank-resembling reality

upward flow field of approximately 1.5 m s<sup>-1</sup> in the tube. The flow within the draft tube was modelled by providing a fixed flow field propelling the fluid upwards with the appropriate velocity. Accurately modelling the impeller would require a substantially finer particle size due to its small size.

The inflow and outflow from the tank were modelled using periodic boundaries with flow fields of the aforementioned speed. This essentially means that the fluid particles leaving the tank are directed to the inlet with their velocities adapted to match the inlet velocity.

As stated in Sect. 1, one of the limitations of SPHASE was the use of periodic boundaries. This resulted in an improper model formulation of the inlet and outlet of the tank as compared to the real digester. While in the real digester the inlet and outlet are both on the same side as seen in Fig. 1b, Rezavand et al. [21] considered them to be on opposite sides of the tank. Also, the outlet in their simulation was a geometrically simplified version of reality. Another assumption made in their work was to model the inlet as being submerged instead of simulating a splashing inlet as found in the real digester. A submerged inlet means that the inlet opens directly into the entirety of fluid, i.e., all the available volume as shown in Fig. 1a which consists of fluid. However, in the case of a splashing inlet, the inlet is maintained at some distance above the fluid surface. This causes the inlet fluid to “splash” onto the fluid surface and requires the free-surface flow modelling in this region. In the first geometry presented, the simplifications mentioned above are applied to ensure homogeneity while validating the simulations.

Since one of the objectives of this study is to study the effect of a draft tube on mixing, a second geometry was prepared without a working draft tube as shown in Fig. 1b. This allows assessing the mixing performance of the digester without external mixing. This geometry also considers the

**Table 1** Simulation parameters used in DSPH

Parameter		Submerged inlet	Splashing inlet		FLUENT [4] Multiphase
			With draft tube	Without draft tube	
Initial interparticle distance $dp$ (m)		0.03	0.005	0.005	–
Artificial viscosity		0.015	0.01	0.01	–
$\delta$ -SPH		Disabled	0.01	0.01	–
Number of particles (or mesh elements)	Fluid	274 957	10 218 822	10 227 368	599 955
	Boundary	11 473	86 937	78 391	–
Physical time simulated (s)		120	5	5	80 min
Computational time (min)		205	1268	805	17 280

previously mentioned “splashing” inlet and thus resembles reality.

There were three cases simulated with the following configurations of the digester;

#### 1. Filled tank (Fig. 1a)

This simulation considers the geometry similar to the previous simulations using SPHASE [21] incorporating their assumptions. It is used to validate the simulation. It makes use of a submerged inlet and a draft tube.

#### 2. Splashing inlet (Fig. 1b)

This simulation corrects some of the erroneous assumptions made in the first case. It represents how the tank is in operation currently, i.e., without the draft tube, with a splashing inlet and the correct geometry of the outlet.

#### 3. Splashing inlet with draft tube

This case combines the previous two simulations. It presents a case where there is a draft tube but instead of having a submerged inlet, there is a splashing inlet. This allows for a comparison of how the velocity zones change as a result of removing the draft tube from the tank.

The SPH scheme for all three cases was solved using velocity Verlet as the time stepping method due to its relatively less computation cost and second-order accuracy. The Wendland kernel was used as the weighting function. For the first simulation, the fluid and the boundaries were discretized into particles in a regular grid with an initial interparticle distance,  $dp$  of 0.03 m. This led to a total of 286 430 particles representing the domain. To reduce the numerical instabilities and to simulate the rheological characteristics of the sludge, artificial viscosity was used with  $\delta$ -SPH enabled. The value of artificial viscosity was determined based on the minimisation of the density variations in the simulations and the results of Rezavand et al. [21]. The fluid was considered to be Newtonian as the total solids content in the sludge is less than 2.5% resulting in the fluid behaving very similar to water. A

total of 120 s were simulated taking approximately 3.5 h of computation time on a GeForce® GTX TITAN V.

The second and the third simulations incorporate free-surface flows. This requires the fluid from the inlet and the free-surface to be well resolved which meant that a higher particle density was to be used. The initial interparticle distance of 0.005 m was chosen resulting in a total of 10 305 759 particles. This led to an exponential increase in numerical effort thus restricting the duration of the simulation to only five physical seconds. However, higher interparticle distance (i.e., fewer particles) led to instabilities in the density field or resulted in the fluid being “stuck” within the inlet pipe and having an erratic flow. The parameters used for all three simulations have been listed in Table 1 and compared with the corresponding information for computational effort of the FLUENT simulation [4].

**Particle refinement** The rate of convergence of the simulation has been shown by plotting the  $L_2$  norm of error [8] while considering both, the Fluent and SPHASE results done by Rezavand et al. [21] as the ground truth. The error was calculated based on the axial velocity at 6 m from the bottom of the tank. Three different interparticle distances, 0.06 m, 0.03 m and 0.015 m were used and the results are plotted in Fig. 2 show an acceptable rate of convergence.

## 4 Results and discussion

### 4.1 Filled tank simulation—validation

As previously mentioned, the following simulation is used to validate the DSPH model with the results published in Rezavand et al. [21]. The contours of the velocity magnitude from DSPH simulations are shown in Fig. 3a and are found to be in good agreement with the reference simulations done with SPHASE by Rezavand et al. [21].

Comparing the DSPH and SPHASE simulations, the velocity contours near the inlet exhibit minor differences.



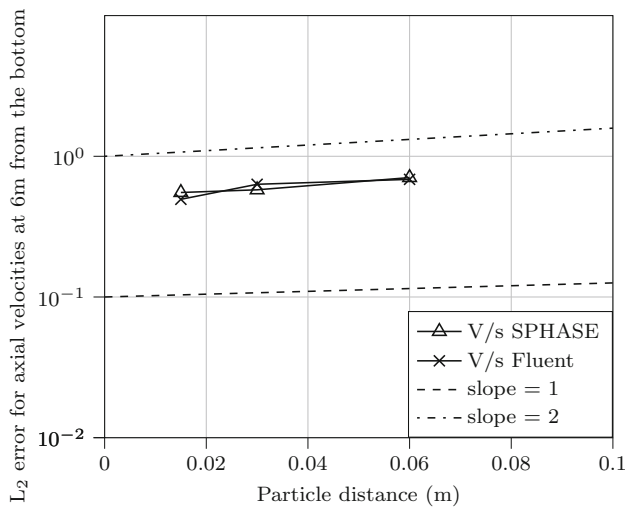


**Fig. 2**  $L_2$  norm of error at different particle resolutions

This is due to the restrictions on how periodic boundaries are implemented in DSPH. The presented simulation required a longer inlet than in the SPHASE simulation as the x-coordinates needed to be aligned with the simulation domain. Regardless, the region at the top of the tank, where the flow from the draft tube and the inlet merge, is well-defined and

shows good agreement with SPHASE simulations. As seen from the velocity contours, it can be argued that the flow from the draft tube, due to its higher velocity compared to the inlet velocity, leads to the formation of a “fluid curtain”. This restricts the fresh fluid from the inlet from interacting with the right section of the tank thereby reducing the quality of mixing with the fresh sludge.

The dominant flow stream of the inlet in the left section of the tank leads likewise to higher flow velocities in this part as corroborated by Fig. 4 This graph shows the velocity plots at the distance of 6 m above the base of the digester, which is a reference height taken to correlate the results with previous work. It can be noted that the velocity profile from DSPH is in good agreement with the SPHASE and FLUENT Simulations by Rezavand et al. [21].

However, an aspect is to be noted: as this is a two-dimensional simulation, the flow pattern deviates slightly from a (more realistic) three-dimensional simulation. For the latter case of a three-dimensional simulation, the additional radial velocity is expected to improve the mixing of the two sections (left and right) which are now completely segregated (see the setup for simulations one and three in Sect. 3).

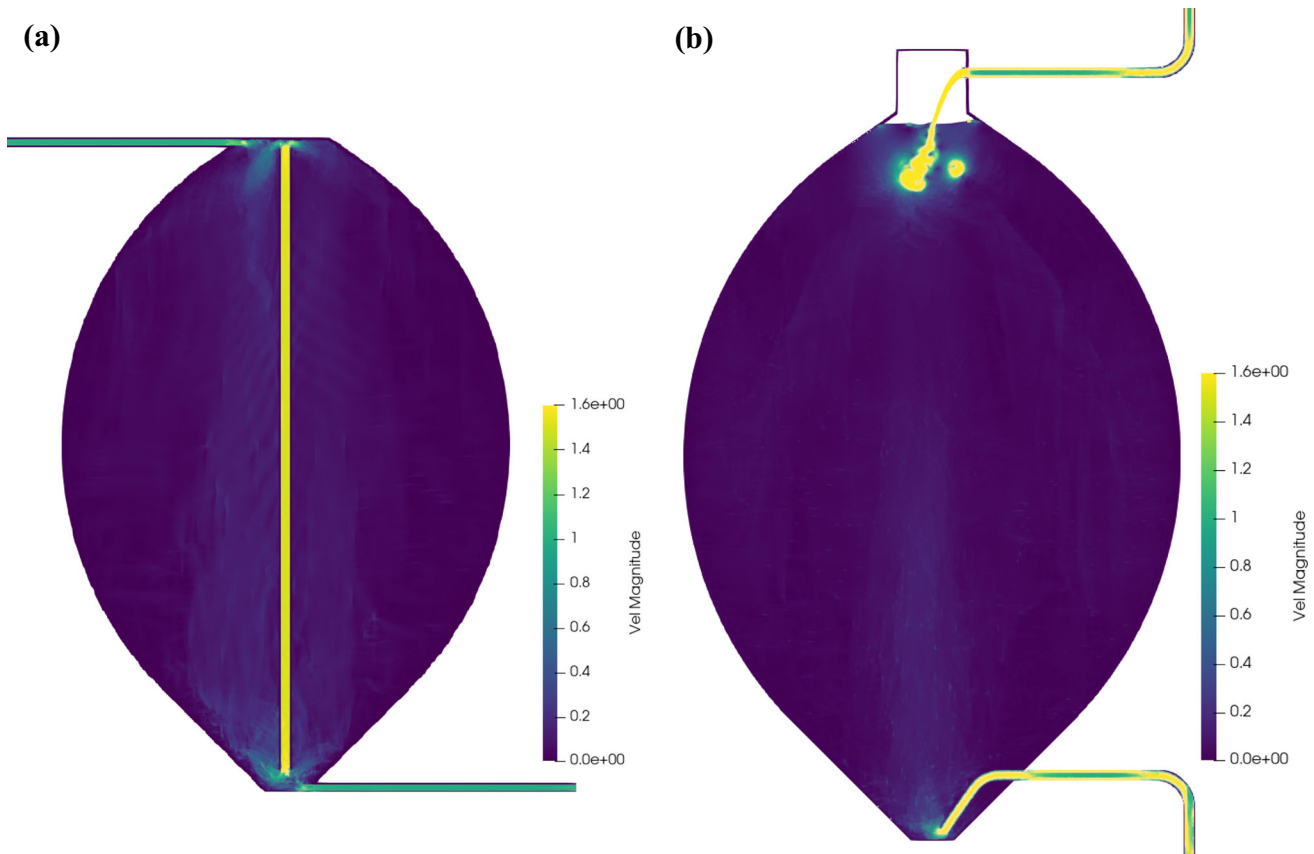


**Fig. 3** Velocity magnitudes ( $\text{m s}^{-1}$ ) of the DSPH model for (a) initial geometry (b) corrected geometry with splashing inlet

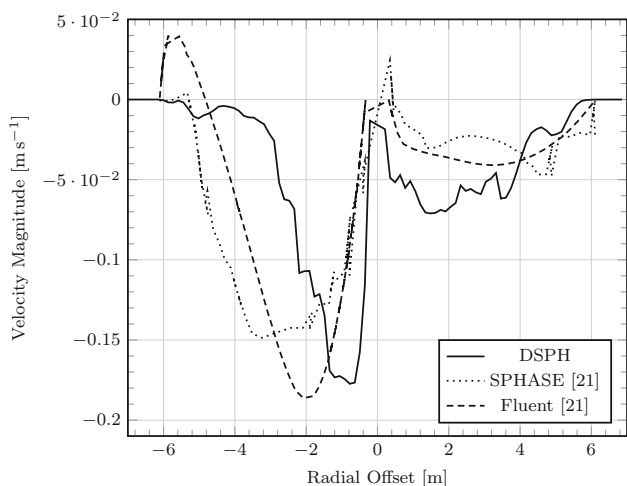


Fig. 4 Axial velocity at 6 m from the bottom of the digester after 120 s

### 4.2 Splashing inlet

This simulation considers the corrected geometry of the tank and the boundary conditions for the inlet. Instead of injecting the fresh fluid directly into the bulk of the fluid already within the tank, the inlet is maintained at an elevation above the fluid surface. This leads to the fluid splashing onto the surface as shown in Fig. 3b. Modelling such an inlet in SPH makes use of the free-surface flows capabilities of the Lagrangian framework. Similar efforts would be a tedious task in Eulerian CFD as it would require computationally intensive transient multiphase simulations.

Figure 5 shows a magnified image of the interaction of the jets from the inlet with the surface. The volume air fraction of a two-phase FLUENT simulation [4] is compared to the free-surface obtained from a DSPH computation after approximately 5 sec. The wider appearance of the jet in Fig. 5a is due to the inclusion of air in the multiphase simula-

tion in FLUENT as opposed to the single phase simulation in DSPH. Despite above, the overall appearance of the profiles is similar, thus further validating the free-surface capabilities of DSPH. The turbulence created due to the splash is visible and propagating through the upper section of the tank and forms a minor recirculation region as seen in Fig. 3b. However, this turbulence is soon dissipated without inducing a huge effect on the mixing at lower regions of the tank. This is due to the large size of the digester and the relatively low inlet velocity.

While in the previous case, mixing results from the gravity driven flow and draft tube, in this scenario, mixing is induced only by the recirculation flow. The splashing inlet induces turbulence in the inflow region, thus reducing the energy of the inflow and consequently resulting in reduced velocities within the digester (see Fig. 6). The upward draft of the fluid is visible on both sides along the walls of the tank. An analogous flow profile has also been presented by Dabiri et al. [4], as shown and compared in Fig. 6, where Ansys FLUENT was used to replicate the effect of splashing inlet. The axial velocities from the two simulations are in good agreement with each other. DSPH predicts the velocity to be lower along the walls of the tanks which is likely attributed to the fact that FLUENT results are from a steady-state simulation, while the SPH simulations are transient over a comparatively short time span of five seconds. It is obvious that such a comparison is far from optimal but extending the DSPH simulation to, e.g., 120 sec would already have increased computation time to an unrealistic 24 days. Despite this shortcoming, the results exhibit a promising agreement.

### 4.3 Splashing inlet with draft tube

This simulation reveals the influence of the draft tube with the correct configuration of the tank as presented in Fig. 1b in

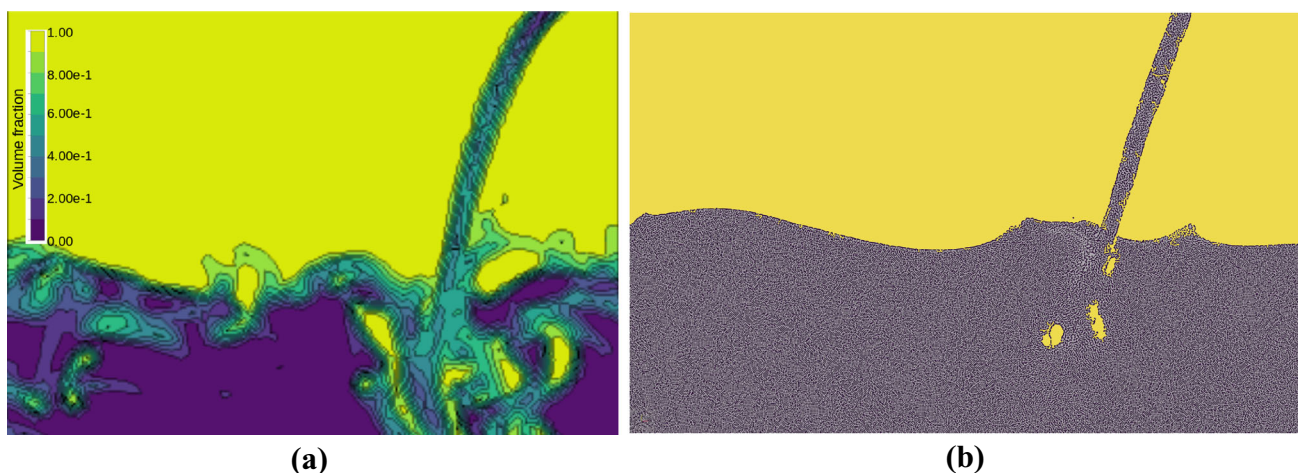
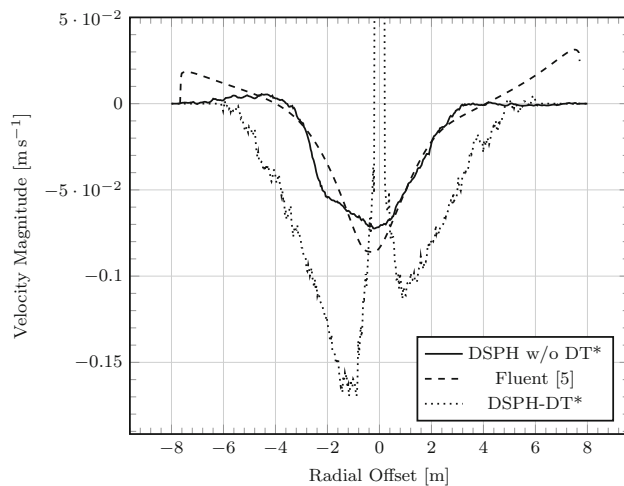


Fig. 5 a Volume air fraction for FLUENT simulation [4] b fluid surface profile for DSPH



**Fig. 6** Comparison of axial velocity at 11.45 m from the bottom for splashing inlet (\*draft tube)

Sect. 3. As observed from the comparison of velocities profiles in Fig. 6, the removal of the mixing device resulted in a significantly lower velocity within the tank. This is accompanied by the downwards flow being largely concentrated in the centre of the tank for the case without the draft tube.

A point of note, however, is the location where the inlet fluid splashes onto the surface of the fluid with respect to the draft tube. In this case, the flow from the inlet is focused on the outlet of the draft tube, which would reduce its effect, but it would also reduce the formation of the fluid curtain which was visible in the earlier simulation. The inlet, in this case, propels the fluid from the draft tube onto the left side of the tank, thus increasing its velocity marginally.

Furthermore, the presented simulation also represents a comparison of the corrected configuration and the initial geometry with the submerged inlet. While the velocity trends are similar, with two segregating sections formed, the simulation in Sect. 4.1 underestimated the velocity on the right side of the tank due to a more even distribution of the fluid between the two sides of the tank.

## 4.4 Mixing properties

### 4.4.1 Low-velocity zones

One of the results of the removal of the draft tube was a reduced overall flow velocity and hence a change in the amount of LVZs. With no external agitation provided, the mixing from a hydrodynamic point of view (i.e., without the consideration of bubble formation induced by bio-processes), depends solely on recirculation, i.e., the inflow of fresh fluid. This results in a lower velocity within the tank and hence a rise in the LVZ and the dead volume as inferred from Table 2.

These results can be compared with the works of Ebner [7]. In his study, tracer measurements were used to estimate the amount of dead volume within the same tank as used in this study without the presence of a draft tube. However, his definition of dead volume only considers the volume of the tank which is used up by sedimentation leading to a reduction in the total capacity. He found that there was virtually no volume (within error limits) lost to sediments for a digester tank cleaned a year prior to when the measurements were made. We do not consider sedimentation as it would again require biokinetic modelling of the sludge and change in material properties based on its composition. Instead, we have considered regions with detrimentally low velocities as dead volume based on previously mentioned literature.

It is important to note that in both the simulations, the amount of dead volume was low enough to be neglected in performance evaluation for the purpose of WWT. Therefore, the use of the more energy-consuming draft tube is redundant. However, within the scope of the study, it is impossible to comment on the (potentially positive) effect of the draft tube on the biokinetic processes as this would require integrated simulation of the AD properties.

### 4.4.2 Lagrangian coherent structures

As mentioned earlier, LCSs allow for the formation of a basic skeletal system along which the fluid develops. These surfaces define stable lines/surfaces within the tank, indicating zones which might have suboptimal interaction with the fresh sludge introduced via the inlet. Figure 7 shows the forward FTLE which denotes the LCSs for the splashing inlet with and without a draft tube.

As expected, due to the low velocities within the tank as compared to the inlet and outlet zones as well as the draft tube, there are no prominent LCSs within the main body of the tank. This implies that there are no significant ridges formed separating the fluid within the main body of the tank. However, the LCS formed close to the inlet and the outlet of the draft tube at the top and the bottom of the tank in Fig. 7 signify the separation of the two sides of the digester as discussed earlier for the velocity profiles.

An important interaction of the draft tube and the outlet is visible from the LCS pattern, the ridges developed due to the draft tube make a barrier for the fluid on the right and restrict its flow into the outlet.

Similar to the FTLE, the vorticity of the fluid provides information on the regions with local rotational flow, hence reducing the effect of mixing in that region. For this purpose, the Q-criterion [12] was used as a measure for vorticity. This measure is able to differentiate between shear and rotational vortices formed within the fluid. A region with a positive value of Q-criterion is dominated by rotational vor-



**Table 2** Comparison of the LVZ and dead volume for with and without draft tube for splashing inlet

Metric	With draft tube (%)	Without draft tube (%)	Experimental (%)
LVZ	16.83	38.21	
Dead volume	0.52	1.20	<1

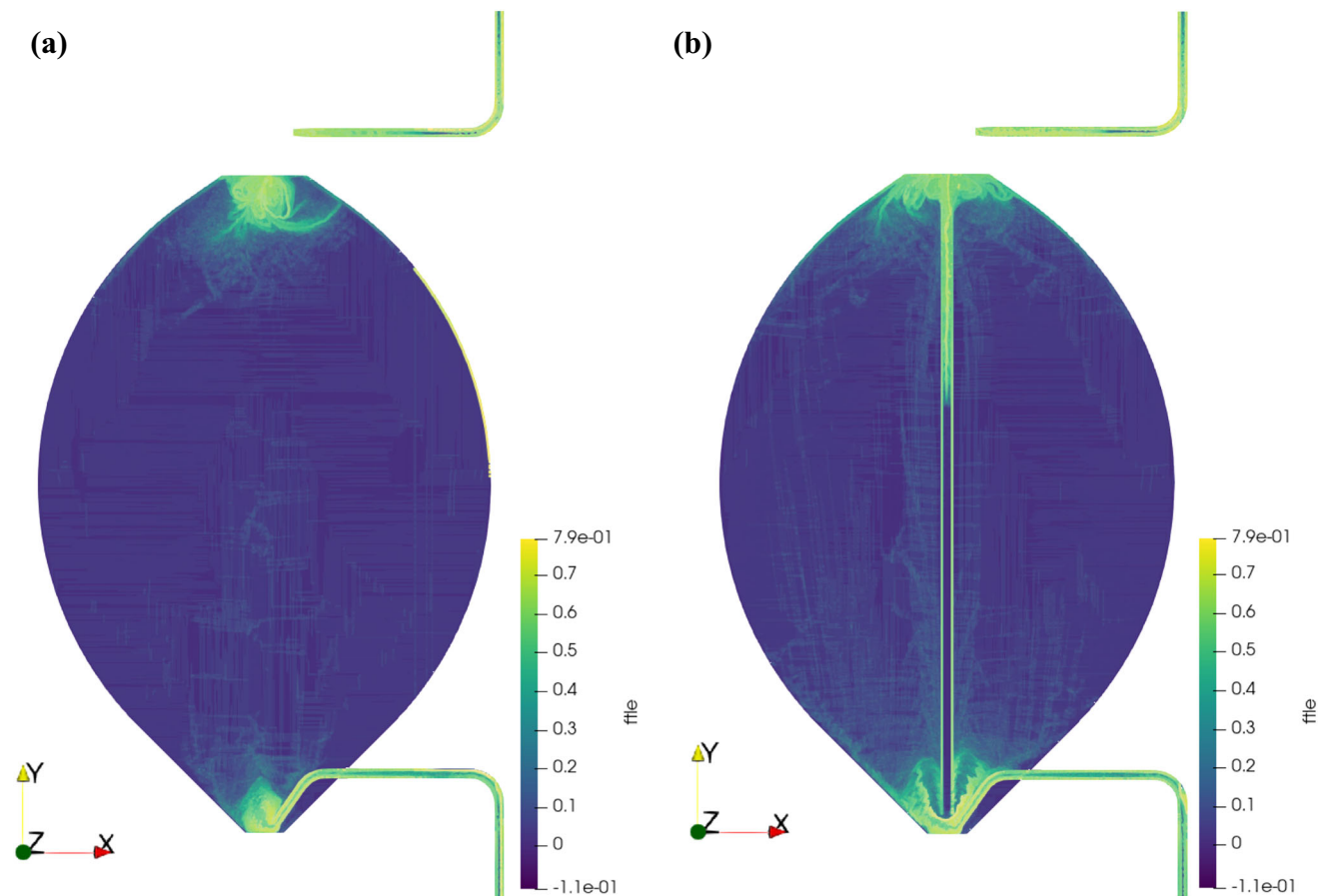


**Fig. 7** Forward FTLE by 5 s representing LCS profiles for splashing inlet **a** without draft tube **b** with draft tube

tices whereas in regions with a negative Q-criteria, shear dominated flow prevails.

Plotting the Q criterion, as shown in Fig. 8, depicts no regions with positive values. However, the region below the splash zone, down to the base of the tank shows negative values which reduce in magnitude along the radial direction. In this region, viscous stress dominated flow is apparent. This behaviour of the fluid results in improved mixing quality as there are no regions of localised and separated vortices.

### 5 Conclusions

This paper demonstrates the use of DSPH for simulating the slow hydrodynamics inside a digester tank that is in operation at a WWT plant in Austria.

Based on the simulations conducted, SPH was found to have certain benefits as compared to Eulerian methods such as;

- the reduced effort of ensuring the quality of the mesh, i.e., pertaining to the wall refinement, skewness, Jacobian, etc.
- possibility to visualise LCS which requires particle based methods.
- ability to represent/track particle (fluid) movement with the time histories being available at any point.
- simulate free-surfaces without using multiphase models.

The last two points are of immense importance considering the flow within the tank and the fact that, as a next step, we aim to couple the hydrodynamics with the biokinetic reactions for AD.

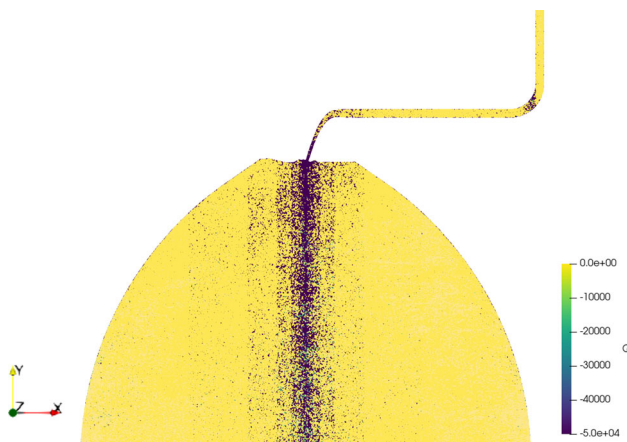


**Fig. 8** Q criterion contour for splashing inlet

In terms of application, we conclude that if the focus of the investigation is solely the hydrodynamics inside the digester, one should resort to standard Eulerian methods and software solutions, such as FLUENT. The reason being that the option of mesh reduction and steady-state simulations allow for reduced computational effort. Focusing additionally (along with hydrodynamics) on biochemical conversions and free-surface flow phenomenon, SPH-based methods become rapidly more attractive.

Further, we investigated the effect of the removal of the mechanical mixing device, in this case, a draft tube, on the mixing conditions within the tank. For that comparison, we applied a commonly used criterion, also used for experimental measurements, i.e., the presence of LVZ and dead volume.

- It was noted that, even though the draft tube leads to the reduction of LVZ by 56%, the velocity values remained well within the required limits to meet the LVZ criteria.
- Although it was a two-dimensional simulation, the amount of dead volume obtained was very similar to the experimental values.

For this case study, we found a limited influence of the implemented draft tube. The removal of which should not affect digester performance significantly. We also studied the presence of LCS which allows us to identify sections within the tank where mixing is insufficient.

One of the main motivations for using Lagrangian methods for digester tank simulations is to obviate the explicit modelling of advection of species when including biokinetic conversion processes in the simulation. Following this addition to the SPH formulation in DSPH, it will be possible to compare the change in methane production as a consequence of operational changes, for example, the removal of the draft tube and to further optimise the operation of such a digester.

**Acknowledgements** This research is part of a project which is supported by the Federal Ministry of the Republic of Austria for Agriculture, Regions and Tourism in collaboration with the Kommunalkredit Public Consulting GmbH [Grant Number: B801259].

**Funding** Open access funding provided by University of Innsbruck and Medical University of Innsbruck.

## Declarations

**Conflict of interest** The authors declare that they have no conflict of interest.

**Open Access** This article is licensed under a Creative Commons Attribution 4.0 International License, which permits use, sharing, adaptation, distribution and reproduction in any medium or format, as long as you give appropriate credit to the original author(s) and the source, provide a link to the Creative Commons licence, and indicate if changes were made. The images or other third party material in this article are included in the article's Creative Commons licence, unless indicated otherwise in a credit line to the material. If material is not included in the article's Creative Commons licence and your intended use is not permitted by statutory regulation or exceeds the permitted use, you will need to obtain permission directly from the copyright holder. To view a copy of this licence, visit <http://creativecommons.org/licenses/by/4.0/>.

## References

1. Batstone DJ, Keller J, Newell RB, Newland M (2000) Modelling anaerobic degradation of complex wastewater. i: model development. *Biores Technol* 75(1):67–74
2. Colin F, Egli R, Lin FY (2006) Computing a null divergence velocity field using smoothed particle hydrodynamics. *J Comput Phys* 217(2):680–692
3. Dabiri S, Noorpoor A, Arfaee M, Kumar P, Rauch W (2021) Cfd modeling of a stirred anaerobic digestion tank for evaluating energy consumption through mixing. *Water* 13(12):1629. <https://doi.org/10.3390/w13121629>
4. Dabiri S, Sappl J, Kumar P, Meister M, Rauch W (2021) On the effect of the inlet configuration for anaerobic digester mixing. *Bio-process Biosyst Eng* 2021:1–14
5. Domínguez JM, Fourtakas G, Altomare C, Canelas RB, Tafuni A, García-Feal O, Martínez-Estévez I, Mokos A, Vacondio R, Crespo AJC et al (2021) Dualsphysics: from fluid dynamics to multiphysics problems. *Comput Part Mech* 2021:1–29
6. DualSPHysics. Dualsphysics/dualsphysics, 2021. <https://github.com/DualSPHysics/DualSPHysics/wiki/3.-SPH-formulation>
7. Christian Ebner. Unpublished report by BioTreat GmbH (2020)
8. Fatehi R, Manzari MT (2011) Error estimation in smoothed particle hydrodynamics and a new scheme for second derivatives. *Comput Math Appl* 61(2):482–498
9. Filho CADF (2017) Development of a computational instrument using a Lagrangian particle method for physics teaching in the areas of fluid dynamics and transport phenomena. *Rev Bras Ensino Física* 39(4):2017. <https://doi.org/10.1590/1806-9126-rbef-2016-0289>
10. Fourtakas G, Dominguez JM, Vacondio R, Rogers BD (2019) Local uniform stencil (lust) boundary condition for arbitrary 3-d boundaries in parallel smoothed particle hydrodynamics (sph) models. *Comput Fluids* 190:346–361. <https://doi.org/10.1016/j.compfluid.2019.06.009>

11. Henze M, Grady CPL, Gujer W, Marais GVR, Matsuo T (1987) Activated Sludge Model No. 1. International Association on Water Pollution Research and Control
12. Huntō JCR, Wray AA, Moin P (1988) Eddies, streams, and convergence. Center for Turbulence Research
13. Karpinska AM, Bridgeman J (2016) Cfd-aided modelling of activated sludge systems—a critical review. *Water Res* 88:861–879
14. Kostoglou M, Karapantsios TD, Matis KA (2007) CFD model for the design of large scale flotation tanks for water and wastewater treatment. *Ind Eng Chem Res* 46(20):6590–6599. <https://doi.org/10.1021/ie0703989>
15. klar. rein. aiz. (2021). <http://www.aiz.at/CMS/>
16. Monaghan JJ (1988) An introduction to SPH. *Comput Phys Commun* 48(1):89–96. [https://doi.org/10.1016/0010-4655\(88\)90026-4](https://doi.org/10.1016/0010-4655(88)90026-4)
17. Monaghan JJ (1992) Smoothed particle hydrodynamics. *Ann Rev Astron Astrophys* 30(1):543–574
18. Le Moulec Y, Potier O, Gentric C, Leclerc JP (2008) Flow field and residence time distribution simulation of a cross-flow gas-liquid wastewater treatment reactor using CFD. *Chem Eng Sci* 63(9):2436–2449. <https://doi.org/10.1016/j.ces.2008.01.029>
19. Qi W-K, Guo Y-L, Xue M, Jing-Ru D, Li W, Li Y-Y (2015) Effect of viscosity on the mixing efficiency in a self-agitation anaerobic baffled reactor. *Bioprocess Biosyst Eng* 38(5):905–910
20. Reece G, Rogers BD, Lind S, Fourtakas G (2020) New instability and mixing simulations using sph and a novel mixing measure. *J Hydrodyn* 32(4):684–698
21. Rezavand M, Winkler D, Sappl J, Seiler L, Meister M, Rauch W (2019) A fully Lagrangian computational model for the integration of mixing and biochemical reactions in anaerobic digestion. *Comput Fluids* 181:224–235
22. Sindall R, Bridgeman J, Carliell-Marquet C (2013) Velocity gradient as a tool to characterise the link between mixing and biogas production in anaerobic waste digesters. *Water Sci Technol* 67(12):2800–2806
23. Sun P, Colagrossi A, Marrone S, Zhang AM (2016) Detection of Lagrangian coherent structures in the sph framework. *Comput Methods Appl Mech Eng* 305(03):849–868. <https://doi.org/10.1016/j.cma.2016.03.027>
24. Terashima M, Goel R, Komatsu K, Yasui H, Takahashi H, Li Y, Noike T (2009) CFD simulation of mixing in anaerobic digesters. *Biores Technol* 100(7):2228–2233. <https://doi.org/10.1016/j.biortech.2008.07.069>
25. Wang H, Larson RA, Borchardt M, Spencer S (2019) Effect of mixing duration on biogas production and methanogen distribution in an anaerobic digester. *Environ Technol* 2019:1–7
26. Winkler D, Meister M, Rezavand M, Rauch W (2016) SPHASE—smoothed particle hydrodynamics in wastewater treatment. In: World Environmental and Water Resources Congress 2016. American Society of Civil Engineers. <https://doi.org/10.1061/9780784479889.032>
27. Winkler D, Meister M, Rezavand M, Rauch W (2017) gpuSPHASE—a shared memory caching implementation for 2d SPH using CUDA. *Comput Phys Commun* 213:165–180. <https://doi.org/10.1016/j.cpc.2016.11.011>
28. Binxin W, Chen S (2008) Cfd simulation of non-Newtonian fluid flow in anaerobic digesters. *Biotechnol Bioeng* 99(3):700–711. <https://doi.org/10.1002/bit.21613>

**Publisher's Note** Springer Nature remains neutral with regard to jurisdictional claims in published maps and institutional affiliations.